Extreme geomagnetic reversal frequency during the Middle Cambrian as revealed by the magnetostratigraphy of the Khorbusuonka section (northeastern Siberia)

Yves Gallet, Vladimir Pavlovic, Igor Korovnikov

Extreme geomagnetic reversal frequency during the Middle Cambrian as revealed by the magnetostratigraphy of the Khorbusuonka section (northeastern Siberia)

Yves Gallet [a], Vladimir Pavlov [b,c], Igor Korovnikov [d]

[a] Université de Paris, Institut de Physique du Globe de Paris, CNRS, Paris, France

[b] Institute of Physics of the Earth, Russian Academy of Science, Moscow, Russia

[c] Kazan Federal University, Kazan, Russia

[d] Trofimuk Institute of Petroleum Geology and Geophysics, Russian Academy of Science, Novosibirsk, Russia

Abstract

We present new magnetostratigraphic results obtained for the Drumian stage (504.5-500.5 Ma; Epoch 3/Middle Cambrian) from the Khorbusuonka sedimentary section in northeastern Siberia. They complement previous data that did not allow the determination of a reliable estimate of the geomagnetic reversal frequency during this time. Magnetization of the samples is carried by a mixture of magnetite and hematite in various proportions. Thermal demagnetization makes it possible to distinguish two magnetization components. The low unblocking temperature (<350°C) component has a steep inclination and likely originates from remagnetization in a recent field. At higher temperatures, the magnetization isolated possesses the two polarities. Its direction is usually well determined; however, for a noticeable set of samples, a strong overlap between the demagnetization spectra of the two components prevents the determination of reliable directions, although their polarities are well established. The directions from 437 samples define a sequence of 78 magnetic polarity intervals,

22 of which are observed in a single sample. Biostratigraphic data available from the Khorbusuonka section indicate that the duration of the studied section is ~3 Myr. A geomagnetic reversal frequency of 26 reversals per Myr is therefore estimated for the Drumian, reduced to 15 reversals per Myr if only the polarity intervals defined by at least two consecutive samples are retained. This is an extreme reversal rate, similar to that obtained for the Late Ediacaran (late Precambrian), ~50 Myr earlier, which has been related to a late nucleation of the inner core. The reversal frequency appears to have drastically dropped for ~3-4 Myr from a value probably >20 reversals per Myr during the Drumian to ~1.5 reversals per Myr during the Furongian/Upper Cambrian. Such a sharp decrease is consistent with a transition at a ~1-Myr timescale, probably caused by threshold effects in core processes, between two geodynamo modes, one characterized by reversals occurring at frequencies ranging from 1 to 5 reversals per Myr, and the other marked by hyperactivity of the reversing process, with reversal rates >15 reversals per Myr.

Keywords : Magnetostratigraphy, Drumian, Middle Cambrian, Magnetic reversal frequency, extreme reversal rate, geodynamo

1. Introduction

The frequency at which the polarity of the geomagnetic field reverses has motivated many studies to focus on the acquisition of new data to scrutinize variations in frequency over time (e.g. Pavlov and Gallet, 2005), on the statistical analysis of polarity reversal sequences (e.g. McFadden, 1984), as well as on the origin of temporal variations in reversal frequency in relation to core and mantle

dynamics (e.g. Besse and Courtillot, 1986; Driscoll and Olson, 2011; Biggin et al., 2012; Hounslow et al., 2018). Two operational modes have been proposed for the geodynamo (McFadden and Merrill, 1995): (i) a regime without geomagnetic polarity reversals over several tens of millions of years, producing events called superchrons; and (ii) a regime marked by polarity reversals occurring at various frequencies over time. For the Phanerozoic Eon, covering the last ~550 Myr, the marine magnetic anomalies available since the Middle Jurassic, together with magnetostratigraphic data obtained from sedimentary outcrops, have revealed the existence of three superchrons spaced ~150 Myr apart (e.g. Pavlov and Gallet, 2005; Biggin et al., 2012). Between these superchrons, the geomagnetic reversal frequency varied from low values of ~1 reversal per Myr to high values of ~5 reversals per Myr (e. g. McFadden and Merrill, 2000).

The analysis of changes in magnetic reversal frequency has led to many proposals or hypotheses. This has particularly been the case for the last 100 Myr, for which the geomagnetic polarity timescale is likely the best established. Nevertheless, different evolutionary models have been suggested, advocating either a more or less complex, non-stationary reversing process since ~83 Ma ago, that is since the end of the normal-polarity Cretaceous superchron (e.g. Mazaud et al., 1983; Gallet and Courtillot, 1995; McFadden and Merrill, 2000 and references therein), a stationary process marked by a jump-like evolution of the mean durations of magnetic polarity intervals estimated over tens of Myr-long segments (Lowrie and Kent, 2004), or a combination of these two processes (Gallet and Hulot, 1997; Hulot and Gallet, 2003). This indeterminacy in the nature of the modulation of the process that causes geomagnetic reversals is problematic for deciphering the interactions between mantle and core dynamics.

More recently, Gallet and Pavlov (2016) proposed a third geodynamo mode characterized by a hyper reversal frequency, with frequencies reaching more than 10-15 reversals per Myr (note that this range of values is much higher than the one previously used by Meert et al. (2016) to define the hyperactive reversal regime, i.e. > 4-6 reversals per Myr). This regime would be distinct from the one characterized by frequencies ranging from ~1 to ~5 reversals per Myr, referred to as the 'normal' reversing mode by Gallet and Pavlov (2016). This idea was based on the observation of two periods marked by reversal rates that were much higher than those known from, for instance, the Miocene, being of the order of ~4-5 reversals per Myr, and so far considered to be high. The first episode of hyper reversal frequency concerns the Middle Jurassic. This has been proposed from analysis of the oldest marine magnetic anomalies measured in the western Pacific (e.g. Tivey et al., 2006 and references therein). According to these authors, the geomagnetic reversal frequency around 160 Ma achieved values as high as ~12-14 reversals per Myr during a period of a few Myr, although this duration remains poorly established. A second episode was dated from the end of the Precambrian, around 550-560 Ma ago. Mainly defined from magnetostratigraphic data obtained from Baltica and its margins, and from Siberia (Popov et al., 2005; Shatsillo et al., 2015; Bazhenov et al., 2016; see also Halls et al., 2015 for data obtained from Canada/Laurentia), this latter is characterized by an extreme reversal frequency of probably >20 reversals per Myr (Bazhenov et al., 2016). Note that this was based on a rough estimate of sedimentation rates in the sections studied.

The hypothesis of a distinct hyperactivity mode of the reversing process would make it possible to account, on one hand, for the fact that the reversal frequency values observed for the two episodes mentioned above are in no way comparable to

99 those of the other periods and, on the other hand, for the probable existence of long
100 stationary segments in the evolution of the duration of the magnetic polarity intervals
101 (Gallet and Hulot, 1997; Hulot and Gallet, 2003; Lowrie and Kent, 2004). Gallet and
102 Pavlov (2016) also suggested that transitions between the three operational
103 geodynamo modes may have occurred on a ~1-Myr timescale, in accordance with
104 rapid core dynamics, whereas their occurrence and time distribution would depend
105 on the thermal conditions prevailing at the core-mantle boundary, driven by mantle
106 dynamics. In this way, this scenario would be consistent with the widely accepted
107 idea that the long-term evolution of magnetic reversal frequency has been modulated
108 by slow (~100-Myr timescale) mantle convection (e.g. McFadden and Merrill, 1984;
109 Courtillot and Besse, 1987; Courtillot and Olson, 2007; Driscoll and Olson, 2011;
110 Pétrélis et al., 2011; Biggin and al., 2012; Hounslow et al., 2018).

111 It should be stressed, however, that the data allowing constraint of the highest
112 -or extreme reversal frequency values remain very few, and with poor age control for
113 the most remarkable episode at the end of the Precambrian. For this reason, we
114 resampled the Middle Cambrian Khorbusuonka section located in northeastern
115 Siberia, which had previously been studied by Gallet et al. (2003). The latter study
116 revealed quite a large number of polarity reversals, defining a frequency of ~6 to ~8
117 reversals per Myr; however, given the large number of magnetic polarity intervals
118 present in this section, the sampling that had been carried out at the time was clearly
119 insufficient to determine a reliable reversal frequency value, and so only a minimum
120 estimate was possible. Thanks in particular to recent investigations (Korovnikov and
121 Tokarev, 2018), this biostratigraphically-precisely-dated section was therefore a
122 prime target for providing a firm constraint on a very high magnetic reversal
123 frequency. In fact, below, we demonstrate that it is extreme.

It is also worth pointing out that this new information should be placed in a more general geophysical perspective, including considering the possible effect of inner-core nucleation on geodynamo behavior (e.g. Driscoll, 2016; Landeau et al., 2017; Lhuillier et al, 2019; Bono et al., 2019), bearing in mind that the beginning of this nucleation could have been as recent as ~600-700 Ma ago (e.g. Olson et al., 2013; Labrosse, 2015; Driscoll, 2016), or the interactions between Earth's different envelopes (e.g. Kirschvink et al., 1997; Meert et al., 2016). The Cambrian was indeed punctuated by several geological events as major as the explosion in faunal diversity (e.g. Kirschvink et al., 1997), attested to in Canada by the Burgess shales dated as Middle Cambrian, or the possible occurrence, in the Lower Cambrian, of an episode of rapid and major true polar wander (Kirschvink et al., 1997; Mitchell et al., 2010).

2. Age and new sampling of the Khorbusuonka section

The section, named Khorbusuonka in the present study, is located along the left bank of the Khorbusuonka River, about 170 km southwest of the city of Tiksi (λ=71° 28' 47'' N; φ=123° 49' 57'' E; northeastern Siberian platform; Fig. 1). Several Lower and Middle Cambrian sections have been studied along this river, involving the identification of five successive sedimentary formations, named, from the oldest to the most recent, Kessyusa (Late Ediacaran-Lower Cambrian), Erkeket (Lower to Middle Cambrian), and Kuonamka, Yunkyulyabit-Yuryakh and Tyuessala, all Middle Cambrian (see description in Korovnikov, 2002; Korovnikov and Tokarev, 2018). Note that Lower and Middle Cambrian refer to Epochs 2 and 3, respectively (e.g. Ogg et al., 2016). In the present study, the magnetostratigraphic investigations were focused on the Yunkyulyabit-Yuryakh Formation and on the lower to basal part of the

149 Tyuessala Formation (Fig. 2). Paleomagnetic sampling was carried out on the
150 section referred to as Section #2 by Korovnikov and Tokarev (2018), being also the
151 same section as that previously studied by Gallet et al. (2003). This contains a
152 complete record of the Yunkyulyabit-Yuryakh Formation over a thickness of ~74 m.
153 The ~85-m-thick part of the section that was sampled consists of alternation of flat-
154 lying limestones and marls of varying colors -grayish, reddish, sometimes greenish
155 (Fig. 2).

156 The dating of the Yunkyulyabit-Yuryakh and Tyuessala formations in the
157 studied section was based on the discovery of trilobites and brachiopods along the
158 entire sedimentary thickness, as well as in the other sections of the Khorbusuonka
159 river. A detailed (and recent) description of the findings has been given in Korovnikov
160 and Tokarev (2018) (see also Gallet et al., 2003 and references therein). Three
161 regional trilobite zones have been documented -*Tomagnostus fissus* over a thickness
162 of ~9 m, *Corynexochus perforatus-Anopolenus henrici* over a thickness of ~22 m and
163 *Anomacarioides limbataeformis* over a thickness of ~54 m. These zones mark the
164 upper part of the Amgan stage (the first 9 m of the section) and the lower part of the
165 Mayan stage (the remaining part of the section; Fig. 2) in the Siberian system
166 (e.g. Krasnov et al., 1983; Korovnikov and Tokarev, 2018). It is worth mentioning that
167 the thickness of the *Anomacarioides limbataeformis* interval in the section
168 investigated corresponds to less than one-third of that of the entire trilobite zone in
169 the area (Korovnikov and Tokarev, 2018).

170 A question has arisen concerning the correlation between the Siberian
171 biostratigraphic scale and the international Geological Time Scale. The situation
172 seems to now have been resolved, whereas it was not at the time of Gallet et al.
173 (2003). The studied section is unambiguously dated as Drumian (ex-Stage 6), as

recognized in the international system and is part of Epoch 3 of the Cambrian (=Middle Cambrian; e.g. Babcock et al., 2007; Howley and Jiang, 2010 and references therein). The beginning of this stage corresponds to the base of *Tomagnostus fissus* because these trilobites appear on the Siberian Platform at the same stratigraphic level as the species called *Ptychagnostus atavus,* which is a key species for defining the lower limit of the Drumian stage (e.g. Babcock et al., 2007; Korovnikov and Tokarev, 2018 and references therein). In the Khorbusuonka section, the base of *Tomagnostus fissus* has been determined in the thin, ~2.5-m-thick Kuonamka Formation, composed of dark gray to black limestones and marls, conformably underlying the Yunkyulyabit-Yuryakh Formation (Korovnikov and Tokarev, 2018). This indicates that the basal part of the Drumian stage is absent from the section that was studied. Similarly, the upper to terminal part of the Drumian stage is absent because the *Lejopyge laevigata* trilobite zone is also absent from the section (the base of this species marks the top of the Drumian).

According to the most recent version of the Geological Time Scale (e.g. Ogg et al., 2016), the Drumian stage lasted 4 Myr, between 504.5 and 500.5 Ma. The Khorbusuonka section, therefore, has a duration of less than 4 Myr, probably of the order of ~3 Myr, although it is difficult to estimate precisely the extent of the missing portions of the *Tomagnostus fissus* and *Anomacarioides limbataeformis* trilobite zones.

During the summer of 2016, we collected a time-series of ~550 hand-samples through the Yunkyulyabit-Yuryakh and Tyuessala formations, with stratigraphic intervals of about 10 to 20 cm between the samples. For comparison, the magnetostratigraphic sequence obtained by Gallet et al. (2003) for the same part of Khorbusuonka Section #2 relied on 119 samples. It should be noted that to the steep

slope (Fig. 1) and the risk of falling rocks made the sampling conditions quite difficult. As a result, samples from the two field works, conducted 15 years apart, could not be located with sufficient accuracy relative to each other to allow us to combine the two data sets into a single one.

3. Paleomagnetic Results

The analyses were carried out in the paleomagnetism laboratories at the Institut de Physique du Globe de Paris and the Institute of Physics of the Earth (Russian Academy of Sciences) in Moscow. In both cases, magnetization measurements were performed using a 2G cryogenic magnetometer installed in a magnetically shielded room. Not surprisingly, the paleomagnetic behavior observed in this study shared all the characteristics previously identified by Gallet et al. (2003) from a smaller collection of samples.

The samples were thermally demagnetized using more than 15 temperature steps. These demagnetizations allowed the isolation of two magnetization components (Fig. 3). A first low unblocking temperature component was isolated at up to 300-350°C. This component shows a steep inclination and clearly has the direction of the present day field at the site (Table 1; Fig. 3, 4a). The characteristic magnetization component was then isolated up to the Curie temperature of magnetite for a set of samples (Fig. 3c,f), and up to the Curie temperature of hematite for the others (Fig. 3a-b,d-e). The magnetization appeared to be carried by a mixture of magnetite and hematite in different proportions, with the same magnetic polarity recorded by the two magnetic phases. This combination of magnetic carriers, evident from the thermal demagnetization of the natural remanent magnetization (NRM; Fig.

3), was confirmed by the thermal demagnetization of three-axis isothermal remanent magnetization (IRM) acquired in three orthogonal directions (Fig. 5; Lowrie, 1990). The high unblocking temperature magnetization component possessed the two magnetic polarities (Fig. 3, 4b). As also shown by Gallet et al. (2003), many samples showed a strong overlap between the demagnetization spectra of the two magnetization components between ~350°C and ~400-500°C, which made it difficult to accurately estimate the direction of the characteristic component for a significant number (~20%) of samples (Fig. 6). In these cases, however, it was possible to determine an approximate direction, which, although biased by the remagnetization (secondary) component, gave clear information about its magnetic polarity. These directions were used to establish the magnetostratigraphic sequence (Fig. 7), but not to estimate a mean direction for each of the two magnetic polarity states (Fig. 4b). The 317 directions that were best determined had maximum angular deviation (MAD) most generally <7.5° (~90% in this category) and <5° for ~67% of the samples in this same category. Despite this selection (after the elimination of 18 deviant directions likely associated with geomagnetic polarity transitions; Fig. S1), the two mean directions of the different polarities were not antipodal at the 95% confidence level (γ=11.3° for γ_c=4.0°; Table 1; McFadden and McElhinny, 1991), likely because of a residual contamination by the remagnetization component (Fig. 4c). Nevertheless, the general mean direction obtained for the high-temperature magnetization component (Table 1) was identical to the mean direction that was previously estimated by Gallet et al. (2003) from a much smaller dataset (γ=2.8° for γ_c=3.4°; McFadden and McElhinny, 1991). It is worth noting that the data from 114 samples were rejected mainly because only the secondary magnetization component in the present-day field direction was recorded or their magnetization directions were too

248 scattered upon heating (Fig. S1a-d). This relatively high number, which represents
249 ~20% of the total collection, is probably related to the very large number of magnetic
250 reversals observed in the studied section (see below). However, a significant number
251 of rejected samples were found in the Tyuessala Formation, showing a lithology
252 generally less favorable for paleomagnetic analyses than that of the Yunkyulyabit-
253 Yuryakh Formation.

254 The two elements that concern, on one hand, the choice of the magnetic
255 polarity of the directions obtained, and on the other hand, the primary nature of the
256 characteristic magnetization isolated at Khorbusuonka are worth discussing (see also
257 discussion in Gallet et al., 2003). Numerous paleomagnetic results have shown that
258 the Siberian Platform was located in the Southern Hemisphere during the Cambrian,
259 rotated by 180° from its current orientation; it then crossed the Equator towards the
260 end of the Middle Ordovician (e.g. Khramov, 1987; Gallet and Pavlov, 1996; Pavlov
261 and Gallet, 2005; Torsvik et al., 2012). As a consequence, paleomagnetic directions
262 with a negative (resp. positive) inclination and a declination of ~160° (resp. ~340°)
263 have a normal (resp. reverse) polarity (Fig. 4b).

264 The primary nature of the characteristic magnetization was deduced from the
265 following evidence: (i) whether predominantly carried by magnetite or hematite, the
266 directions of the magnetization component are similar and the geomagnetic polarity
267 does not depend on the predominant magnetic phase in the samples. This showed
268 that the hematite likely has an early diagenetic (or detritic?) origin; (ii) most of the 18
269 abnormal (or deviating) directions isolated through the section are observed at the
270 transition between two magnetic polarity intervals (Fig. S1e-f). These most likely
271 reflect a transitional configuration of the geomagnetic field during a polarity reversal;
272 (iii) the mean direction estimated for the Khorbusuonka section (note that the

273 averaging tended to reduce the bias due to the recent magnetic field) is almost
274 identical at the 95% confidence level to the tilt-corrected mean direction (and after its
275 transfer to the location of the Khorbusuonka section) previously obtained by Pavlov
276 and Gallet (2001) for the Middle Cambrian part of the Kulumbe section, located
277 nearly 1500 km away (γ=3.7°; γ_c=3.5°; McFadden and McElhinny, 1991). In contrast
278 the two mean directions are significantly different before bedding correction (γ=16.0°;
279 γ_c=3.6°; McFadden and McElhinny, 1991), which gives a positive, albeit partial, fold
280 test. It is also worth mentioning that the Kulumbe section is slightly younger than the
281 Khorbusuonka section, since the lower part of the Kulumbe section has been dated
282 as being at the top of the Drumian *Anomacarioides limbataeformis* trilobite zone (e.g.
283 Pavlov and Gallet, 2005; Kouchinsky et al., 2008); and (iv) the paleomagnetic pole
284 defined from the characteristic component isolated at Khorbusuonka is different from
285 all other paleomagnetic poles of younger age known for the Siberian Platform (e.g.
286 Khramov, 1987; Torsvik et al., 2012).

287

288 **4. Discussion and conclusions**

289 The results described above indicate that the Khorbusunka section contains a
290 record of the geomagnetic field that prevailed during the Drumian stage (Epoch
291 3/Middle Cambrian). The new data offer an average resolution gain of 3.7 compared
292 to the results of Gallet et al. (2003) (i.e. the ratio between the 437 new samples and
293 the 119 samples used by Gallet et al., 2003). This gain varied according to the
294 trilobite zones, from ~3.4 for the *Tomagnostus fissus* zone, to ~2.9 for the
295 *Corynexochus perforatus-Anopolenus henrici* and ~4.1 for the *Anomacarioides*
296 *limbataeformis* zone. They show the occurrence of 78 magnetic polarity intervals
297 along the 85 m of the studied section, of which 22 intervals were defined by only one

sample (Fig. 7). An extreme, but probably simplistic, approach would be to eliminate the latter intervals by considering them too uncertain, which would then imply a sequence of 46 magnetic polarity intervals; however, there is no a priori reason why the directions of the samples concerned should be considered to be less well defined than the others. The most likely reason for the intervals defined by a single sample is that they were very short and the sampling rate was still too low compared to the prevailing geomagnetic reversal frequency. For the same stratigraphic sequence, Gallet et al. (2003) found 42 magnetic polarity intervals, with 18 intervals defined by a single sample, or a series of 18 intervals after the exclusion of the latter. An important observation is that, despite the very significant difference in the number of polarity intervals found between these two studies, a fairly convincing correlation can be observed between the two magnetostratigraphic sequences (Fig. 8).

A comparison is reported in Fig. 8 between the Khorbusuonka results and those found in a section sampled along the Kulumbe river (Pavlov and Gallet, 2001). This section was dated by the presence of the *Anomacarioides limbataeformis* and *Lejopyge laevigata* trilobite zones: that is, it covers the top of the Drumian and the lower part of the Guzhangian stage (ex-stage 7; e.g. Ogg et al., 2016). In the Kulumbe section, there was a strong contrast between the *Anomacarioides limbataeformis* zone, marked by numerous geomagnetic reversals, and the *Lejopyge laevigata* zone, with only a few geomagnetic reversals detected. It was not possible to achieve a convincing correlation between the Khorbusuonka and Kulumbe sequences (Fig. 8). A first option would be that this difficulty primarily results from the large number of polarity reversals observed in both Drumian sections, a difficulty further amplified by possible sampling rate effects and/or due to differences in sedimentation rate between the two sections. The second would be that the Kulumbe

section is slightly younger than the Khorbusuonka section (see also Pavlov and Gallet, 2005). The most important point, however, is that, whatever the option retained, the data from Kulumbe confirm the presence of numerous magnetic polarity reversals during the *Anomacarioides limbataeformis* zone of the Drumian stage.

Based on the chronostratigraphic timescale considered for the Cambrian (e.g. Ogg et al., 2016), and on the biostratigraphic data available for the Middle Cambrian deposits found along the Khorbusuonka river, the duration of the Khorbusuonka section analyzed in the present study would have a duration of ~3 Myr. This relatively short duration implies a geomagnetic reversal frequency as high as ~26 reversals per Myr, if all polarity intervals are considered, or 15 reversals per Myr if the intervals defined by a single sample are excluded. Even considering a misinterpretation of some of the magnetic polarity intervals defined by a single sample, it follows that the geomagnetic reversal frequency during the Drumian stage was likely >20 reversals per Myr. This is obviously an extreme reversal rate, if we refer, for example, to the evolution of the geomagnetic reversal frequencies over the last 100 million years. In addition, the new paleomagnetic data show that, during this period of hyperactivity of the reversing process, the geometry of the geomagnetic field probably remained essentially dipolar, with the slight non-antipodality of the two directions of opposite polarity observed at Khorbusuonka being likely due to a residual contamination by the recent field (Fig. 4c).

The extreme geomagnetic reversal frequency observed at Khorbusuonka appears very similar to that found by Bazhenov et al. (2016) for the Zigan Formation in the southern Urals (Russia), dated to the late Precambrian (Late Ediacaran), some 50-60 Myr before the Drumian. Furthermore, as in Khorbusuonka, the Late Ediacaran data also showed that a dipolar field likely prevailed at that time. Beyond these

348 exceptional reversal rates, there is the question of their evolution throughout the
349 Cambrian and the geophysical implications that could result from it.
350 Magnetostratigraphic data obtained from Siberia, Australia and China have provided
351 constraints on that evolution after the Drumian; more precisely, during the terminal
352 part of the Middle Cambrian (Guzhangian stage), the Furongian Epoch/Upper
353 Cambrian and during the Ordovician (see synthesis in Pavlov and Gallet, 2005 and
354 Hounslow, 2016). The Kulumbe sequence showed about 30 geomagnetic polarity
355 intervals during the Guzhangian, but it should be noted that this sequence is very
356 preliminary due to the poor quality of the paleomagnetic signal observed in the rocks
357 of the Orakta Formation (Kouchinsky et al., 2008). Considering a duration of ~3.5
358 Myr for the Guzhangian stage (Ogg et al., 2016), the reversal frequency would have
359 reached a value of ~10 reversals per Myr at the end of the Middle Cambrian. In
360 contrast, the reversal frequency would have been much lower during the Furongian
361 Epoch/Late Cambrian (~1.5 reversal per Myr), with ~15 to 20 magnetic polarity
362 intervals over a duration of ~12 Myr (Pavlov and Gallet, 2005; Kouchinsky et al.,
363 2008; Ogg et al., 2016; Hounslow, 2016). A similar low reversal rate would also have
364 prevailed at the beginning of the Lower Ordovician, just before the onset of the
365 reverse-polarity Moyero Superchron (Fig. 9; Gallet and Pavlov, 1996; Pavlov and
366 Gallet, 1998; 2005; Pavlov et al., 2017). Therefore, the presently available
367 magnetostratigraphic data show that the magnetic reversal frequency dramatically
368 dropped from values >20 reversals per Myr to ~1.5 reversal per Myr in ~3-4 Myr,
369 which is the duration of the Guzhangian stage (with an 'intermediate', albeit high,
370 value of ~10 reversals per Myr during the Guzhangian).

371 The new magnetostratigraphic data, and those previously obtained by
372 Bazhenov et al. (2016), next raise the question of the evolution in reversal frequency

373 during the Lower Cambrian. Was the period between ~550 Ma and ~500 Ma
374 characterized by a single or more episodes of hyperactivity in the reversing process?
375 Note further that the onset of the hyperactivity episode in the Late Ediacaran has not
376 yet been documented. To date, the magnetostratigraphic data available for the Lower
377 Cambrian are neither numerous nor constrained enough to answer this question with
378 certainty. Even though the data mainly obtained from Siberia (Kirschvink and
379 Rozanov, 1984; Kirschvink et al., 1991; Gallet et al., 2003) and China (Duan et al.,
380 2018 and references therein) clearly showed the occurrence of many geomagnetic
381 polarity reversals during Epoch 2/the Lower Cambrian, it remains difficult to precisely
382 determine the reversal rates. Duan et al. (2018) recently proposed a frequency of ~7
383 reversals per Myr between ~524 Ma and 514 Ma, but the stratigraphic sequence
384 from which the data were obtained was fragmentary; it therefore seems possible (but
385 not proven) that the reversal frequency was actually higher during this period. The
386 Lower Cambrian paleomagnetic data obtained at Khorbusuonka by Gallet et al.
387 (2003) also attest to a very high geomagnetic reversal frequency during the
388 Tommotian and Atdabanian (Gallet et al., 2003 tentatively proposed a reversal
389 frequency even higher than that of the Drumian), in addition to the occurrence of a
390 major true polar wander event near the end of the Lower Cambrian, in agreement
391 with Kirschvink et al. (1997). The data, however, should be confirmed by further
392 studies on other sedimentary sections in Siberia or elsewhere. At this stage, it is only
393 possible to affirm that the reversal frequency was high (>5 reversals per Myr) during
394 the Lower Cambrian, but the hyperactivity character (>15 reversals per Myr) cannot
395 be established (Fig. 9).

396 Comparing dipole field behavior in numerical simulations with varying inner-
397 core size and assuming inner-core nucleation began during the Neoproterozoic,

Lhuillier et al. (2019) recently suggested that the hyperactivity of the reversing process during the latest Precambrian and the Cambrian could be linked to a critical size of the inner core, around an aspect ratio of ~0.2. During this critical period, corresponding to significant changes in the flow pattern in the tangent cylinder, the reversal frequency would have been very sensitive to variations in the vigor of the convection in the outer core. If these simulations do indeed provide relevant information for the geodynamo, this sensitivity could account for long duration of the hyperactivity phenomenon, if it persisted for about 50 Myr, or recurrence of such events, if several hyperactivity episodes were present, a very different situation from that observed during the Middle Jurassic (Lhuillier et al., 2019). It should be noted, however, that just changing the thermal conditions at the core-mantle boundary can alone account for the full spectrum of temporal variations in geomagnetic reversal rate (e.g. Driscoll and Olson, 2011; Olson et al., 2013). On another hand, Bono et al. (2019) showed that the hyperactivity episode at the end of the Precambrian was also accompanied by very low mean paleointensity. This observation would be consistent with a weak-field geodynamo state before inner-core nucleation as predicted by numerical models (Driscoll, 2016; Landeau et al., 2017; see also Bono et al., 2019). Accurate paleointensity data are not yet available to determine whether this state still prevailed in the Middle Cambrian. An important point of note, however, is that both the data from Ediacaran (Bazhenov et al., 2016) and the Middle Cambrian seem to argue for a dipole-dominated field geometry at the beginning of the inner-core growth.

The Cambrian thus appears to be a period marked by remarkable and fascinating phenomena affecting all terrestrial envelopes. Linking them together exceeds the objectives of our study (see for example Kirschvink et al., 1997; Meert et

al., 2016). Here, we have emphasized the exceptional nature of the reversing process during the Middle Cambrian, but the sharp decrease in reversal rate at the end of the Middle Cambrian provides further important information on the geodynamo behavior. It argues for threshold effects in core processes (see also Courtillot and Olson, 2007), which would be consistent with a ~1-Myr-scale transition between two reversing modes; that is, between the normal and hyperactive reversing modes defined by Gallet and Pavlov (2016) (Fig. 9).

Acknowledgements

This study was financed by grants #14.Z50.31.0017 (field work) and #14.Y26.31.009 (laboratory measurements at IPE) of the Ministry of Science and High Education of the Russian Federation, by the INSU-CNRS program PNP and by the Simone and Cino Del Duca Foundation of the French Academy of Science. I.K. was partly financed by grant # 18-05-00285 of the Russian Foundation for Basic Research. We are grateful to Dmitry Gavryushkin for his help on the field. We also thank two anonymous reviewers for their helpful comments on the manuscript. VP benefited from the invitation program of IPGP. This is IPGP contribution no. 4056.

References

Babcock, L. E., Robison, R. A., Rees, M. N., Peng, S., Saltzman, M. R., 2007. The global boundary stratotype section and point (GSSP) of the Drumian stage (Cambrian) in the Drum Mountains, Utah, USA. Episodes 30, 85-95.

Bazhenov, M. L., Levashova, N. M., Meert, J. G., Golovanova, I. V., Danukalova, K. N., Fedorova, N. M., 2016. Late Ediacaran magnetostratigraphy of Baltica: evidence

447 for magnetic field hyperactivity?. Earth Planet. Sci. Lett. 435, 124-135.

448 Biggin, A., Steinberger, B., Aubert, J., Suttie, N., Holme, R., Torsvik, T., van der
449 Meer, D., van Hinsbergen, D., 2012. Possible links between long-term geomagnetic
450 variations and whole-mantle convection processes, Nature Geoscience 5, 526-533.

451 Bono, R. K., Tarduno, J. A., Nimmo, F., Cottrell, R. D., 2019. Young inner core
452 inferred from Ediacaran ultra-low geomagnetic field intensity. Nature Geoscience 12,
453 143-147.

454 Cogné, J.-P., 2003. PaleoMac: A MacIntosh@ application for treating paleomagnetic
455 data and making plate reconstructions. Geochem. Geophys. Geosyst. 4, 1007.

456 Courtillot, V., Besse, J., 1987. Magnetic field reversals, polar wander, and Core-
457 Mantle coupling, Science 237, 1140-1147.

458 Courtillot, V., Olson, P., 2007. Mantle plumes link magnetic superchrons to
459 Phanerozoic mass depletion events. Earth Planet. Sci. Lett. 260, 495–504.

460 Driscoll, P. E., Olson, P., 2011. Superchron cycles driven by variable core heat flow,
461 Geophys. Res. Lett. 38(9), L09304.

462 Driscoll, P. E., 2016. Simulating 2 Ga of geodynamo history. Geophys. Res. Let. 43,
463 1-8.

464 Duan, Z., Liu, Q., Li, L., Deng, X., Liu, J., 2018., Magnetic reversal frequency in the
465 Lower Cambrian Niutitang Formation inferred from Ciye 1 Hole, Hunan Province,
466 South China. Geophys. J. Int. 214, 1301-1312.

467 Gallet, Y., Courtillot, V., 1995. Geomagnetic reversal behaviour since 100 Ma, Phys.
468 Earth Planet. Inter. 92, 235-244.

469 Gallet, Y., Pavlov, V., 1996. Magnetostratigraphy of the Moyero river section

(northwestern Siberia): constraints on geomagnetic reversal frequency during the early Paleozoic. Geophys. J. Int. 125, 95–105.

Gallet, Y., Hulot, G., 1997. Stationary and non-stationary behaviour within the geomagnetic polarity time scale. Geophys. Res. Lett. 24, 1875–1878.

Gallet, Y., Pavlov, V., Courtillot, V., 2003. Magnetic reversal frequency and apparent polar wander of the Siberian platform in the earliest Palaeozoic, inferred from the Khorbusuonka river section (northeastern Siberia). Geophys. J. Int. 154, 829–840.

Gallet, Y., Pavlov, V.E., 2016. Three Distinct Reversing Modes in the Geodynamo. Izvestiya Physics of the Solid Earth 52(2), 291–296.

Halls, H.C., Lovette, A., Hamilton, M., Söderlund, U., 2015. A paleomagnetic and U-Pb geochronology study of the western end of the Grenville dyke swarm: Rapid changes in paleomagnetic field direction at ca. 585 Ma related to polarity reversals ?, Precambrian Research 257, 137-166.

Hounslow, M. W., 2016. Geomagnetic reversal rates following Palaeozoic superchrons have a fast restart mechanism. Nature Communications 7, 12507.

Hounslow, M. W., Domeler, M., Biggin, A. J., 2018. Subduction flux modulates the geomagnetic polarity reversal rate. Tectonophysics 742-743, 34-49.

Hulot, G., Gallet, Y., 2003. Do superchrons occur without any palaeomagnetic warning? Earth Planet. Sci. Lett. 210, 191–201.

Khramov, A. N., 1987. Paleomagnetology. Tarling D. H. (Ed.), Springer-Verlag Berlin Heidelberg, 308 pp.

Kirschvink, J. L., Rozanov, A. Yu, 1984. Magnetostratigraphy of lower Cambrian strata from the Siberian platform: a palaeomagnetic pole and a preliminary polarity

493 time-scale. Geol. Mag. 121, 189-203.

494 Kirschvink, J. L., Magaritz, M., Ripperdam, R. L., Zhuralev, A. Y., Rozanov, A. Y.,
495 1991. The Precambrian/Cambrian boundary: magnetostratigraphy and carbon
496 isotopes resolve correlation problems between Siberia, Morocco and South China.
497 GSA Today 1, 69-71.

498 Kirschvink, J. L., Ripperdam, R. L., Evans, D. A., 1997. Evidence for a large-scale
499 reorganization of Early Cambrian continental masses by inertial interchange true
500 polar wander. Science 277, 541-545.

501 Korovnikov, I. V., 2002. New data on biostratigraphy of the Lower and Middle
502 Cambrian series in the Northeastern Siberian platform. Russ. Geol. Geophys. 43,
503 826-836.

504 Korovnikov, I. V., Tokarev, D. A., 2018. New data on biostratigraphy of the Middle
505 Cambrian section at the Khorbusuonka river, Northeastern Siberian platform. Stratig.
506 Geol. Correl. 26, 599-610.

507 Kouchinsky, A., Bengtson, S., Gallet, Y., Korovnikov, I., Pavlov, V., Runnegar, B.,
508 Shileds, G., Veizer, J., Young, E., Ziegler, K., 2008. The SPICE carbon isotope
509 excursion in Siberia: a combined study of the upper Middle Cambrian-lowermost
510 Ordovician Kulyumbe river section, northwestern Siberian platform. Geol. Mag. 145,
511 609-622.

512 Krasnov, V. I., Savitsky, V. E., Tesakov, Yu I., Khomentovsky, V. V. (Eds),
513 1983. Resolution of the All-Union Stratigraphic Conference on Precambrian,
514 Paleozoic, and Quaternary of Central Siberia. Part 1. Upper Proterozoic (Upper
515 Precambrian) and Lower Paleozoic) [in Russian]. Izd. SNIIGGIMS, Novosibirsk
516 Russia, 215 pp.

517 Labrosse, S., 2015. Thermal evolution of the core with a high thermal conductivity.
518 Phys. Earth Planet. Inter. 247, 36-55.

519 Landeau, M., Aubert, J., Olson, J., 2017. The signature of inner-core nucleation on
520 the geodynamo. Earth Planet. Sci. Lett. 465, 193-204.

521 Lhuillier, F., Hulot, G., Gallet, Y., Schwaiger, T., 2019. Impact of inner-core size on
522 the dipole field behavior of numerical dynamo simulation. Geophys. J. Int. 218, 179-
523 189.

524 Lowrie, W., 1990. Identification of ferromagnetic minerals in a rock by coercivity and
525 unblocking temperature properties. Geophys. Res. Lett. 17, 159–162.

526 Lowrie W., Kent, D., 2004. Geomagnetic polarity timescales and reversal frequency
527 regimes, in: Timescale of the paleomagnetic field, Geophysical Monograph Series
528 145, AGU, 117-129.

529 Mazaud, A., Laj, C., de Sèze, L., Verosub, K., 1983. 15 m.y. periodicity in the
530 frequency of geomagnetic reversals. Nature 304, 328-330.

531 McFadden, M., 1984. Statistical tools for the analysis of geomagnetic reversal
532 sequence. J. Geophys. Res. 89, 3363-3372.

533 McFadden, P., McElhinny, M., 1990. Classification of the reversal test in
534 palaeomagnetism. Geophys. J. Int. 103, 725–729.

535 McFadden, P., Merrill, R., 1995. Fundamental transitions in the geodynamo as
536 suggested by paleomagnetic data, Phys. Earth Planet. Inter. 91, 253-260.

537 McFadden, P., Merrill, R., 2000. Evolution of the geomagnetic reversal rate since 160
538 Ma: Is the process continuous?, J. Geophys. Res. 105, 28,455-28,460.

539 Meert, J. G., Levashova, N. M., Bazhenov, M. L., Landing, E., 2016. Rapid changes

of magnetic field polarity in the late Ediacaran: linking the Cambrian evolutionary radiation and increased UV-B radiation. Gondwana Res. 34, 149-157.

Mitchell, R. N., Evans, D. A., Killian, T. M.~~?~~, 2010. Rapid Early Cambrian rotation of Gondwana. Geology 38, 755-758.

Ogg, J. G., Ogg, G., Gradstein, F. M., 2016. A concise geological time scale 2016. Elsevier Publ., 240 pp.

Olson, P., Deguen, R., Hinnov, L.A., Zhong, S., 2013. Controls on geomagnetic reversals and core evolution by mantle convection in the Phanerozoic. Phys. Earth Planet. Inter. 214, 87–103.

Pavlov, V., Gallet, Y., 1998. Upper Cambrian to Middle Ordovician magnetostratigraphy from the Kulumbe river section (northwestern Siberia). Phys. Earth Planet. Inter. 108, 49–59.

Pavlov, V., Gallet, Y., 2001. Middle Cambrian high magnetic reversal frequency (Kulumbe River section, northwestern Siberia) and reversal behaviour during the Early Palaeozoic, Earth Planet. Sci. Lett. 185, 173–183.

Pavlov, V., Gallet, Y., 2005. A third superchron during the Early Paleozoic. Episodes 28 (2), 78-84.

Pavlov, V.E., Tolmacheva, T.Y., Veselovskiy, R.V., Latyshev, A. V., Fetisova, A. M., Bigun, I. V., 2017. Magnetic stratigraphy of the Ordovician in the lower reach of the Kotuy River: the age of the Bysy-Yuryakh stratum and the rate of geomagnetic reversals on the eve of the superchron. Izvestiya, Physics of the Solid Earth 53, 702-713.

Pétrélis, F., Besse, J., Valet, J.-P., 2011. Plate tectonics may control geomagnetic reversal frequency. Geophys. Res. Lett. 38, L19303.

564 Popov, V.V., Khramov, A.N., Bachtadse, V., 2005. Palaeomagnetism, magnetic
565 stratigraphy, and petromagnetism of the Upper Vendrian sedimentary rocks in the
566 sections of the Zolotitsa River and in the Verkhotina Hole, Winter Coast of the White
567 sea, Russia, Russian J. Earth Sci. 7(2), 1-29.

568 Shatsillo, A.V., Kouznetsov N.B., Pavlov V.E., Fedonkin M.A., Priyatkina N.S., Serov
569 S.G., Rud'ko, S.V., 2015. First magnetostratigraphic data on stratotype of the Lopata
570 Fm (northeast of the Enisey Range): problems of its age and of paleogeography of
571 the Siberian platform at the Proterozoic-Phanerozoic boundary, Doklady Academii
572 Nauk 465 (4), 1-5.

573 Tivey, M.A., Sager, W.W., Lee, S.-M., Tominaga, M., 2006. Origin of the Pacific
574 Jurassic Quiet Zone, Geology, 34(9), 789-792.

575 Torsvik, T. H., Van der Voo, R., Preeden, U., Mac Niocaill, C., Steinberger, B.,
576 Doubrovine, P. V., Douwe, van Hinsbergen, D. J. J., Domeier, M., Gaina, C., Tohver,
577 E., Meert, J. G., McCausland, P. J., Cocks, L. R. M., 2012. Phanerozoic polar
578 wander, paleogeography and dynamics. Earth Science Rev. 114, 325–368.
579

580

581 **Table and Figures captions**

582

583 **Table 1.** Paleomagnetic results obtained from the Drumian part of the Khorbusuonka
584 section. LTC and HTC refer to the magnetization components isolated in the low and
585 high unblocking temperature ranges.

586

587 **Fig. 1.** General geology of northeastern Siberia (a) and of the area in the vicinity of
588 the Khorbusuonka section (b). The red square in panel (a) and the red star in panel
589 (b) indicate the location of the studied Khorbusuonka section.

590

591 **Fig. 2.** View of the Khorbusuonka section analyzed in the present study (@Yves
592 Gallet). The simplified lithology, and the dating of the studied sequence, are from
593 Korovnikov and Tokarev (2018).

594

595 **Fig. 3.** Representative examples of the thermal demagnetization of the samples from
596 the Khorbusuonka section. Solid (resp. open) circles are in the horizontal (resp.
597 vertical) plane. The corresponding magnetization moment versus temperature curves
598 are also reported (right panels).

599

600 **Fig. 4.** Stereographic projections of the directions obtained in the Khorbusuonka
601 section. Directions at the sample level were isolated for the low (a) and high (b)
602 unblocking temperature components (LTC and HTC, respectively). (c) Mean

603 directions with opposite polarities. The closed (open) symbols refer to directions in
604 the lower (upper) hemisphere. All directions were obtained using the PaleoMac
605 software (Cogné, 2003).

606

607 **Fig. 5.** Thermal demagnetization of three-axis isothermal remanent magnetization
608 components acquired in fields of 1.9 T (dots), 0.3 T (triangles) and 0.15 T (squares).
609 These examples show that the magnetization of the samples was likely carried by
610 various mixtures of magnetite and hematite.

611

612 **Fig. 6.** Examples of thermal demagnetization of samples from the Khorbusuonka
613 section showing a strong overlap between the low and high unblocking temperature
614 magnetization components. In these cases, a direction could not be reliably
615 determined for the high unblocking temperature component (see text). Same
616 conventions as in Fig. 3-4.

617

618 **Fig. 7.** Magnetostratigraphy of the Drumian sequence of the Khorbusuonka section.
619 The dark green dots show the directions used to estimate a mean high unblocking
620 temperature magnetization direction, whereas those in light green color refer to
621 biased directions, allowing constraint of only the associated magnetic polarity (see
622 text).

623

624 **Fig. 8.** Comparison between the magnetostratigraphic sequences of Middle
625 Cambrian age (Epoch 3) obtained from the Khorbusuonka (Gallet et al., 2003; this
626 study) and Kulumbe (Pavlov and Gallet, 2001) sections.

627

628 **Fig. 9.** Synthesized sketch of the evolution in geomagnetic reversal frequency since
629 the end of the Precambrian (modified from Gallet et Pavlov, 2016).

630

631 **Supplementary material**

632 **Fig. S1.** (a-d) Thermal demagnetization of rejected samples. In each case, the
633 directional data are reported in orthogonal and stereographic projections, together
634 with the evolution of magnetization as a function of temperature (see text). Same
635 conventions as in Fig. 3 and 4. (e-f) Two examples of demagnetization behavior for
636 samples located at a geomagnetic polarity transition.

637

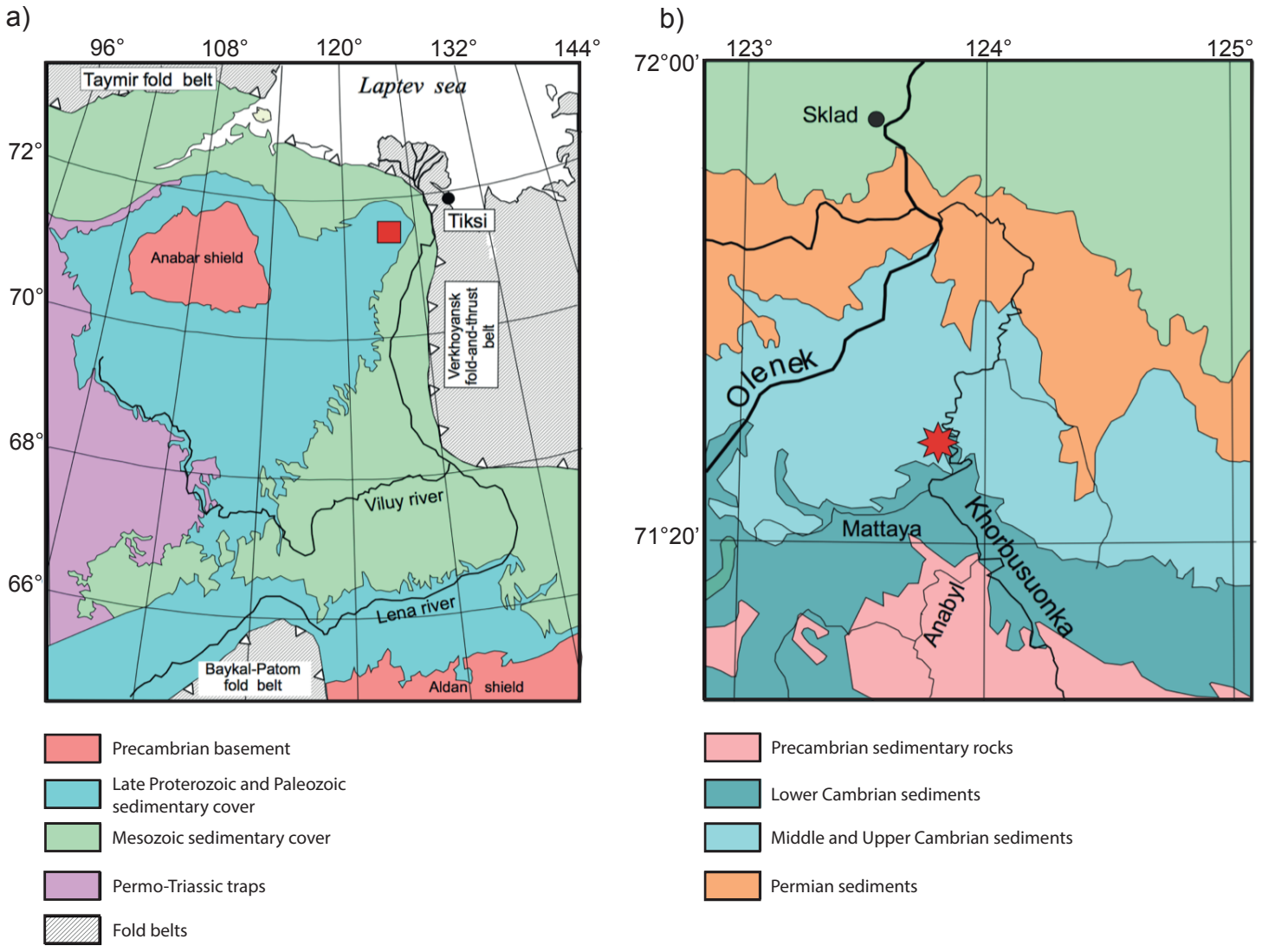
a)
96°
108°
120°
132°
144°
72°
70°
68°
66°
Taymir fold belt
Laptev sea
Tiksi
Anabar shield
Verkhoyansk fold-and-thrust belt
Viluy river
Lena river
Baykal-Patom fold belt
Aldan shield
b)
123°
124°
125°
72°00'
71°20'
Sklad
Olenek
Mattaya
Khorbusuonka
Anabyl
Precambrian basement
Late Proterozoic and Paleozoic sedimentary cover
Mesozoic sedimentary cover
Permo-Triassic traps
Fold belts
Precambrian sedimentary rocks
Lower Cambrian sediments
Middle and Upper Cambrian sediments
Permian sediments

Figure 1

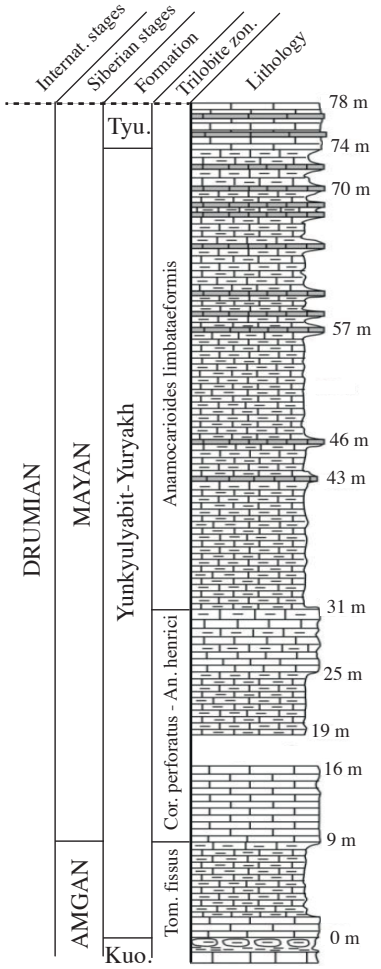
Internat. stages
Siberian stages
Formation
Trilobite zon.
Lithology
DRUMIAN
MAYAN
AMGAN
Tyu.
Yunkyulyabit-Yuryakh
Kuo.
Anamocarioides limbataeformis
Cor. perforatus - An. henrici
Tom. fissus
78 m
74 m
70 m
57 m
46 m
43 m
31 m
25 m
19 m
16 m
9 m
0 m

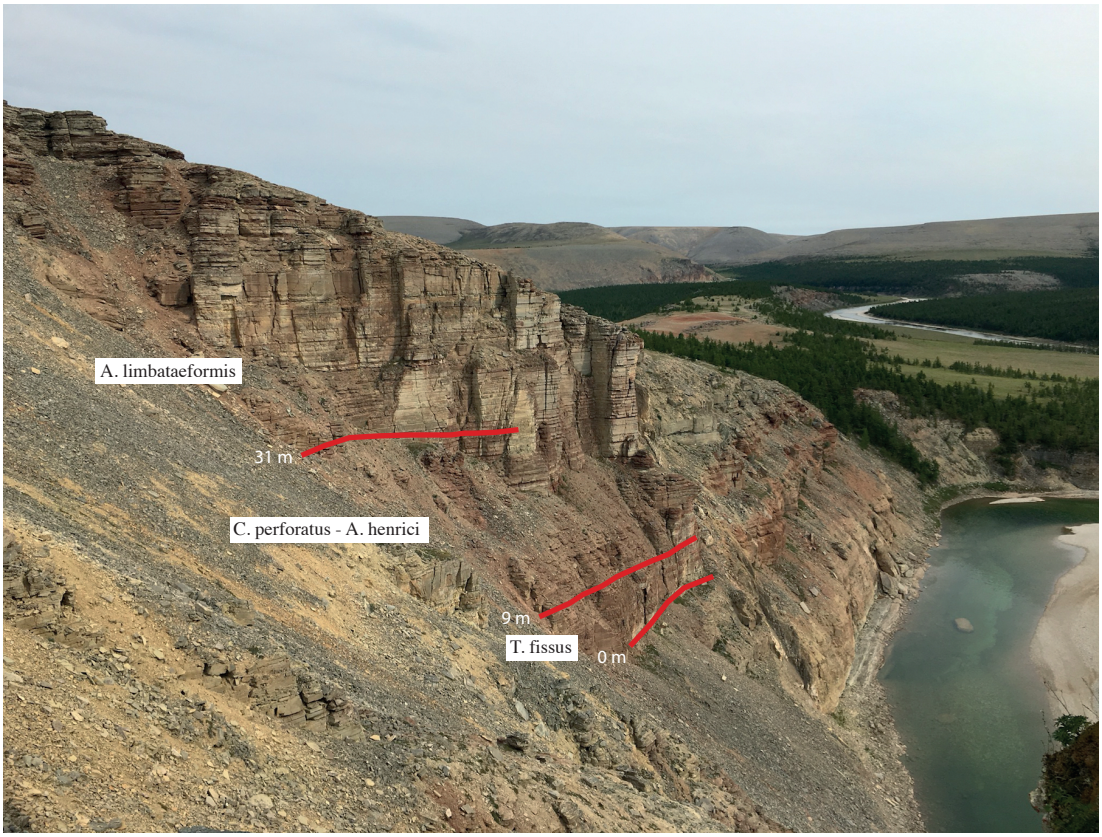
A. limbataeformis
31 m
C. perforatus - A. henrici
9 m
T. fissus
0 m

Figure 2

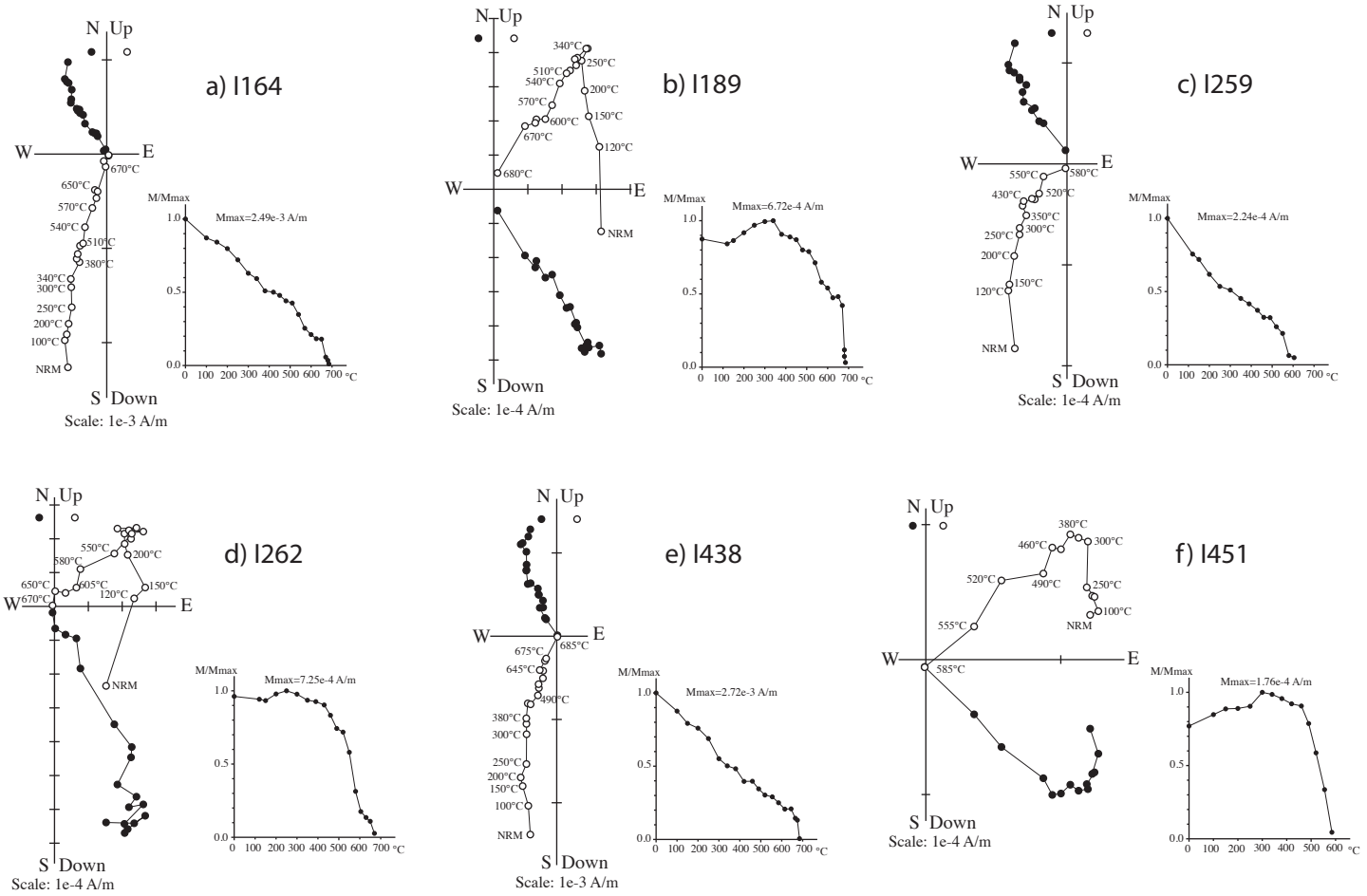
a) I164
N Up
W
E
S Down
670°C
650°C
570°C
540°C
510°C
380°C
340°C
300°C
250°C
200°C
100°C
NRM
M/Mmax
Mmax=2.49e-3 A/m
Scale: 1e-3 A/m
b) I189
N Up
W
E
S Down
340°C
250°C
510°C
540°C
200°C
570°C
600°C
150°C
670°C
120°C
680°C
NRM
M/Mmax
Mmax=6.72e-4 A/m
Scale: 1e-4 A/m
c) I259
N Up
W
E
S Down
550°C
580°C
430°C
520°C
350°C
300°C
250°C
200°C
150°C
120°C
NRM
M/Mmax
Mmax=2.24e-4 A/m
Scale: 1e-4 A/m
d) I262
N Up
W
E
S Down
550°C
200°C
580°C
650°C
605°C
150°C
670°C
120°C
NRM
M/Mmax
Mmax=7.25e-4 A/m
Scale: 1e-4 A/m
e) I438
N Up
W
E
S Down
685°C
675°C
645°C
490°C
380°C
300°C
250°C
200°C
150°C
100°C
NRM
M/Mmax
Mmax=2.72e-3 A/m
Scale: 1e-3 A/m
f) I451
N Up
W
E
S Down
380°C
460°C
300°C
520°C
490°C
250°C
100°C
NRM
555°C
585°C
M/Mmax
Mmax=1.76e-4 A/m
Scale: 1e-4 A/m

Figure 3

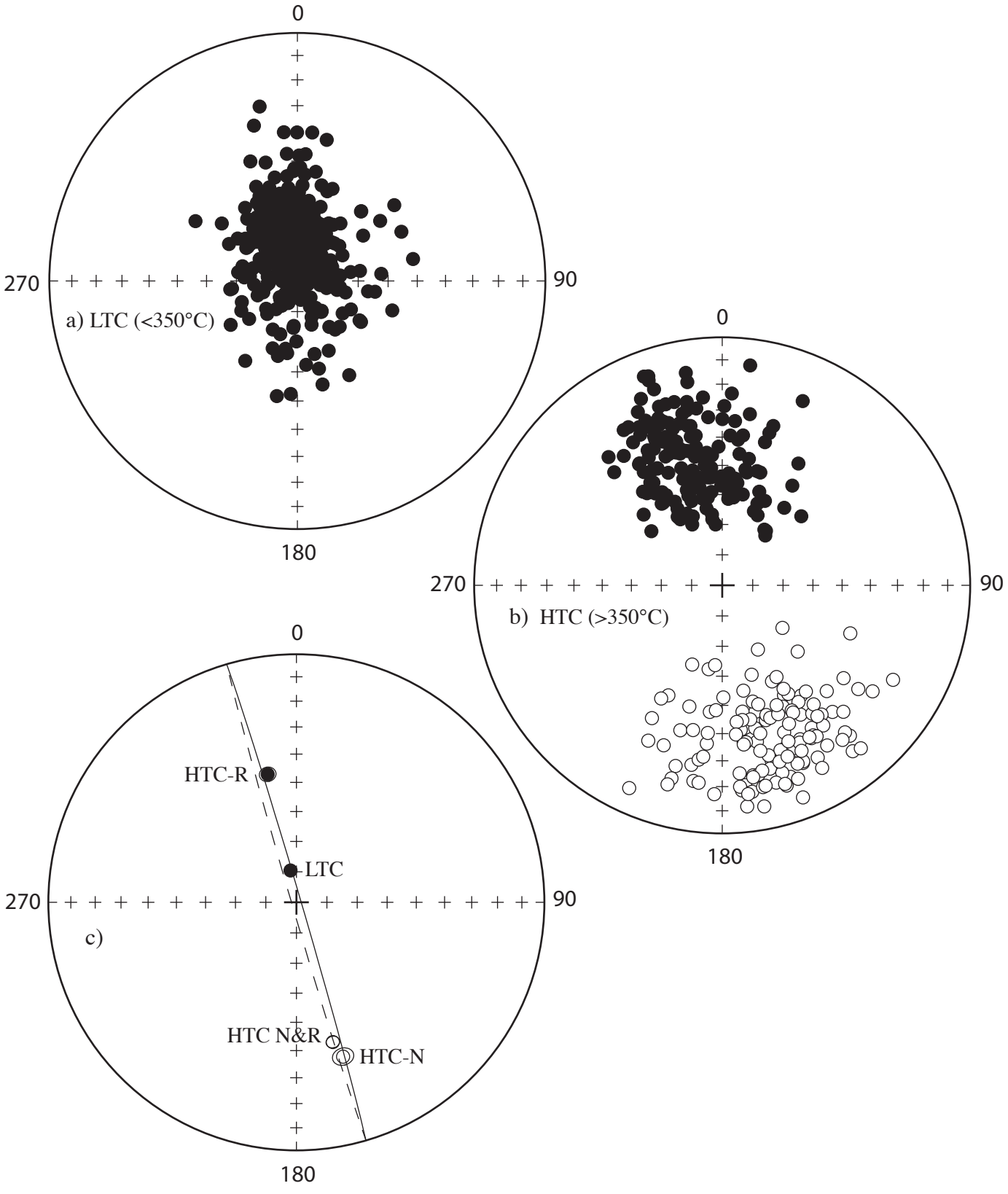
0
270
90
180
a) LTC (<350°C)
0
270
90
180
b) HTC (>350°C)
0
270
90
180
c)
HTC-R
LTC
HTC N&R
HTC-N

Figure 4

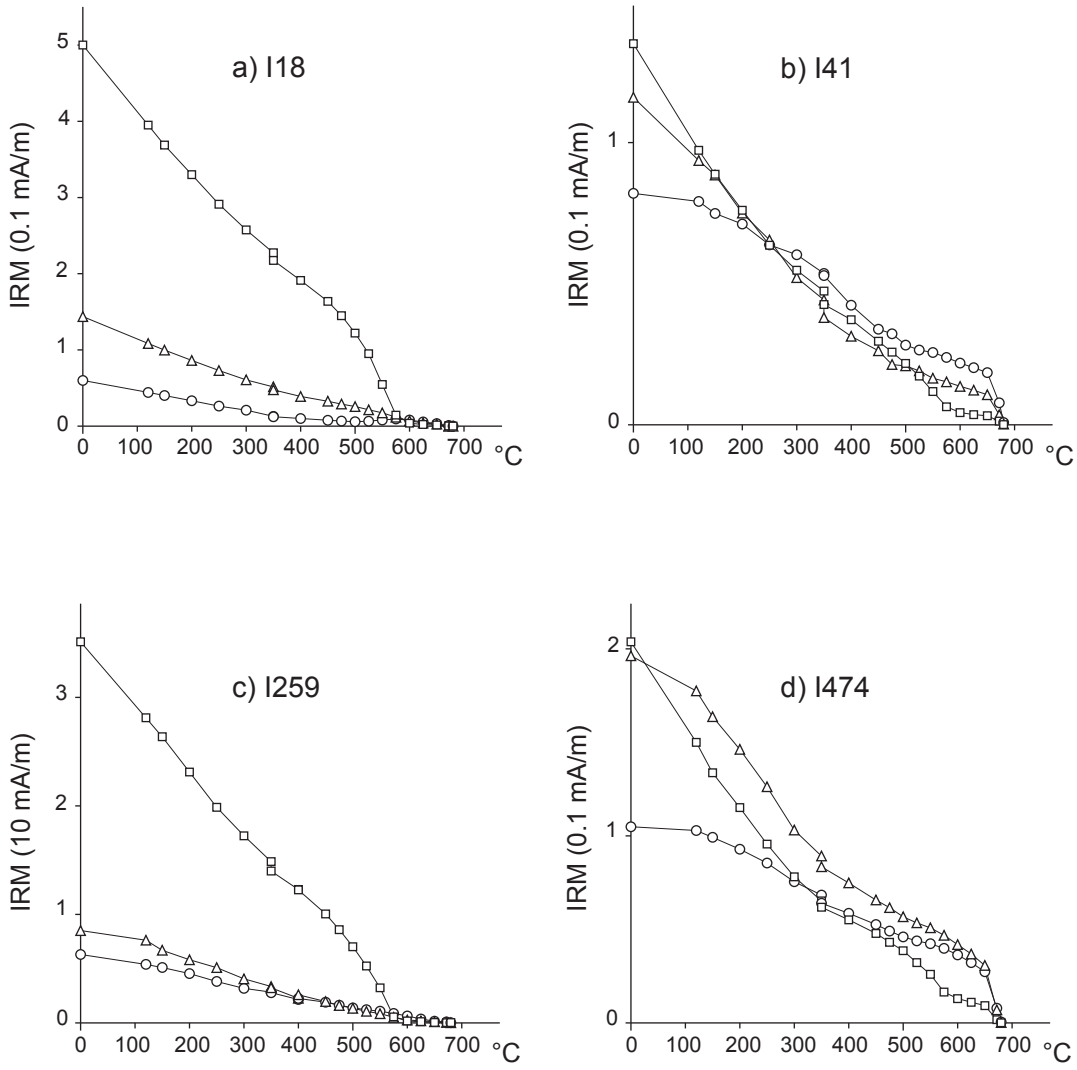
a) I18
b) I41
c) I259
d) I474
IRM (0.1 mA/m)
IRM (10 mA/m)
°C
0
100
200
300
400
500
600
700

Figure 5

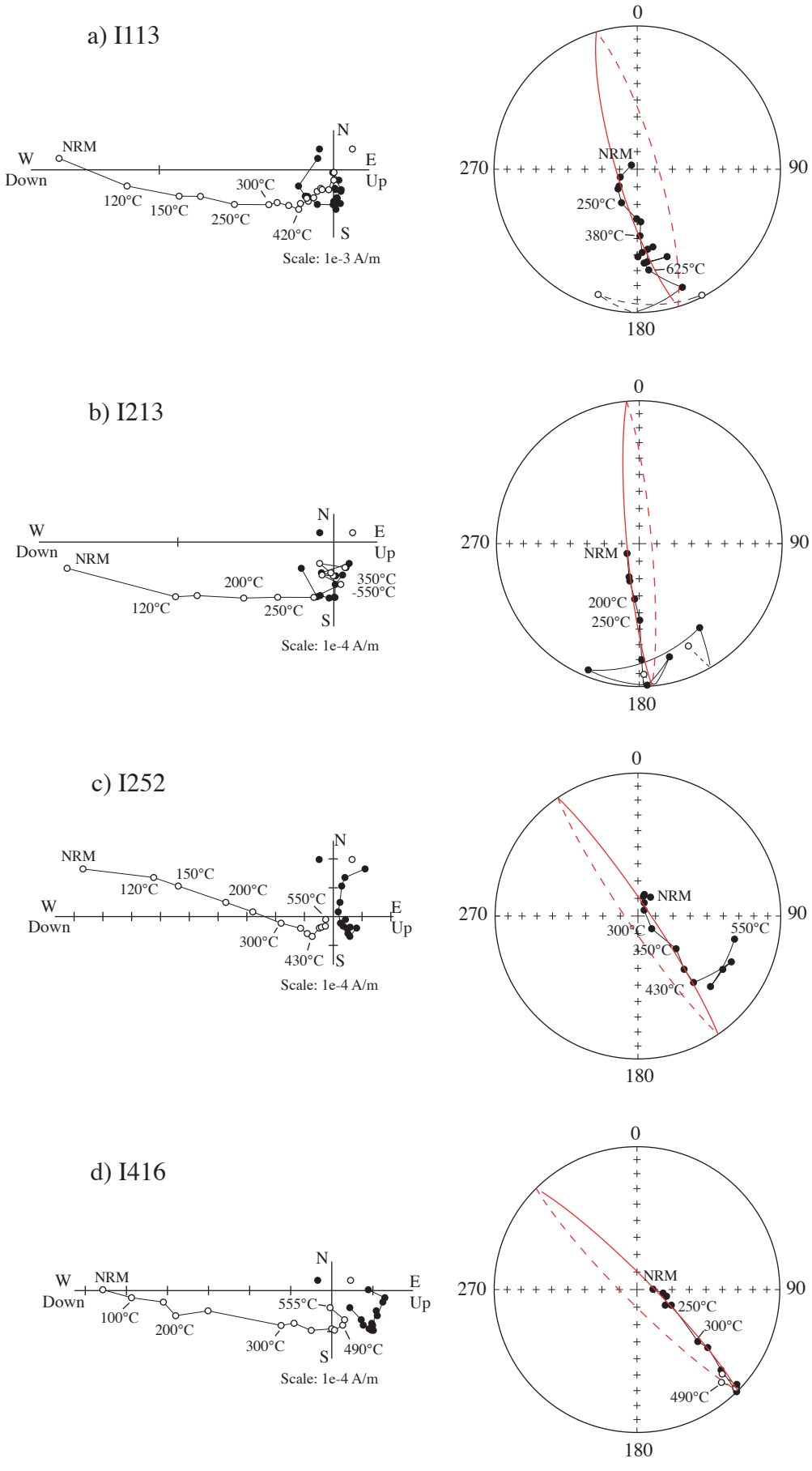
a) I113
N
W
NRM
E
Down
Up
300°C
120°C
150°C
250°C
420°C
S
Scale: 1e-3 A/m
0
270
90
NRM
250°C
380°C
625°C
180
b) I213
N
W
E
Down
Up
NRM
200°C
350°C
-550°C
120°C
250°C
S
Scale: 1e-4 A/m
0
270
90
NRM
200°C
250°C
180
c) I252
N
NRM
150°C
120°C
200°C
550°C
W
E
Down
Up
300°C
430°C
S
Scale: 1e-4 A/m
0
270
90
NRM
300°C
550°C
350°C
430°C
180
d) I416
N
W
NRM
E
Down
Up
555°C
100°C
200°C
300°C
490°C
S
Scale: 1e-4 A/m
0
270
90
NRM
250°C
300°C
490°C
180

Figure 6

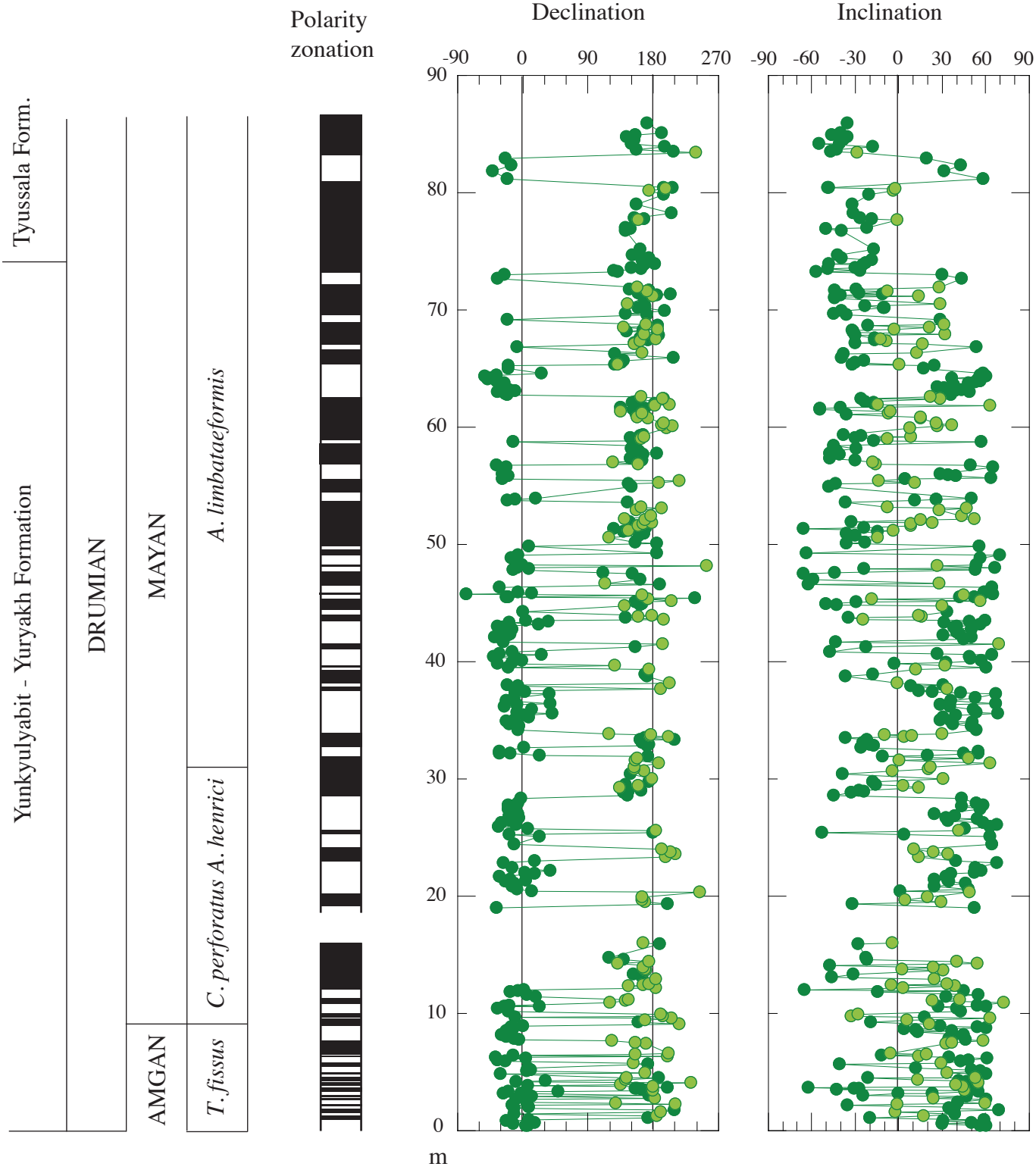
Yunkyulyabit - Yuryakh Formation
Tyussala Form.
DRUMIAN
MAYAN
AMGAN
A. limbataeformis
C. perforatus A. henrici
T. fissus
Polarity zonation
Declination
Inclination
-90 0 90 180 270
-90 -60 -30 0 30 60 90
90 80 70 60 50 40 30 20 10 0
m

Figure 7

Khorbusuonka
(this study)
Khorbusuonka
(Gallet et al., 2003)
Yunkyulyabit - Yuryakh Formation
Tyuessala F.
A. limbataeformis
C. perforatus A. henrici
T. fissus
10 m
A. limbataeformis
C. perforatus
A. henrici
T. fissus
100 m
L. laevigata
A. truncata
A. limbataeformis
Labaznaya Formation
Ust-Brus Formation
Kulumbe
(Pavlov et Gallet, 2001)

Figure 8

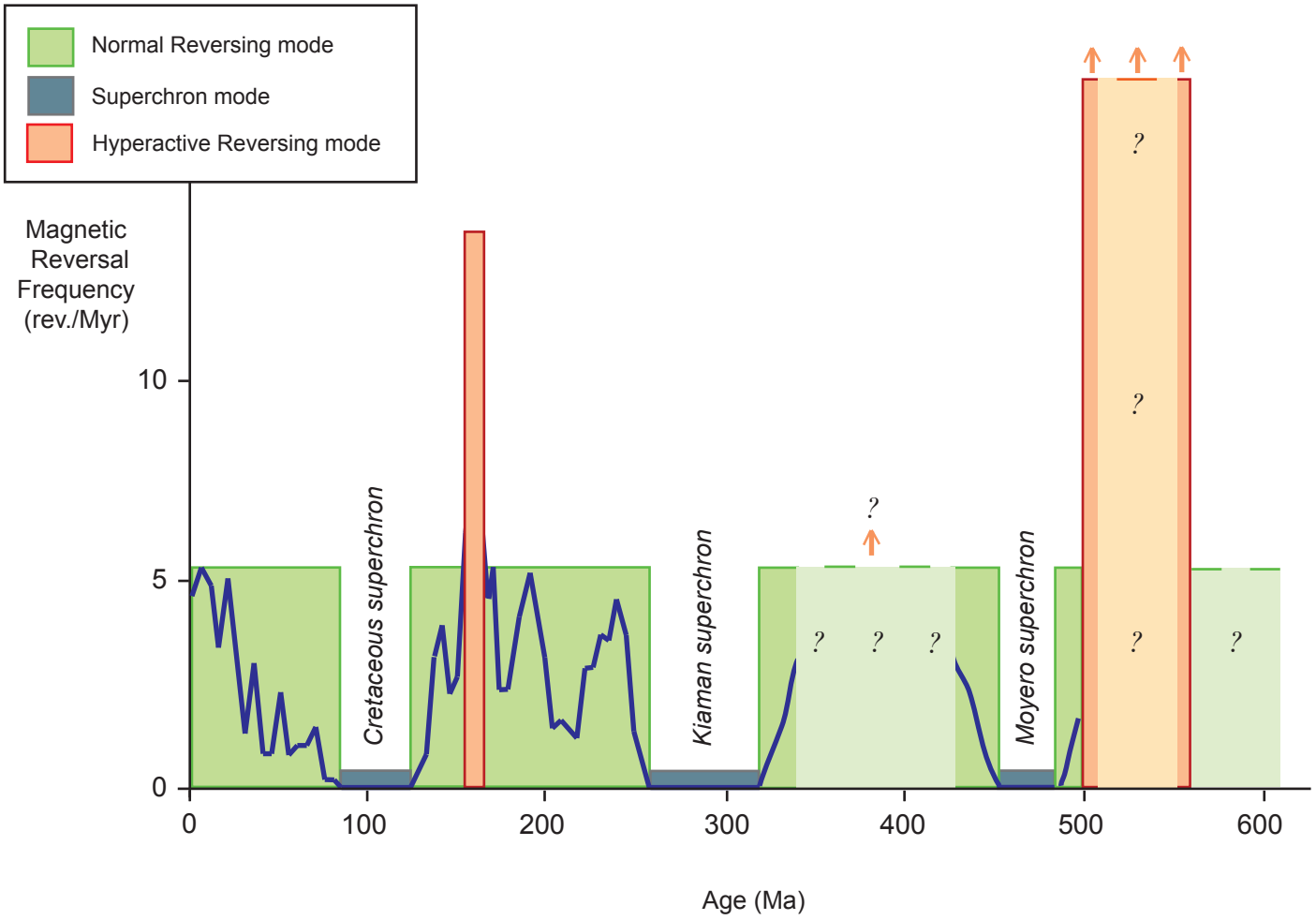
Normal Reversing mode
Superchron mode
Hyperactive Reversing mode
Magnetic Reversal Frequency (rev./Myr)
10
5
0
Cretaceous superchron
Kiaman superchron
Moyero superchron
?
?
?
?
?
?
?
?
?
0
100
200
300
400
500
600
Age (Ma)

Figure 9

Khorbusuonka section λ=71°28'47''N Φ=123°49'57''E	N	In situ				Tilt corrected				Paleomagnetic pole		
		Dec°	Inc°	K	α_{95}	Dec°	Inc°	K	α_{95}	Lat°	Long°	dp°/dm
LTC	515	349.5	79.4	27.5	1.2°	349.6	79.4	27.5	1.2			
HTC-Normal	131	163.1	-35.2	16.4	3.1	163.1	-35.3	16.4	3.1			
HTC-Reverse	168	347.4	46.1	19.3	2.5	347.4	46.1	19.3	2.5			
HTC N+R	299	165.3	-41.4	16.6	2.1	165.4	-41.4	16.6	2.1	-41.6	141.8	1.6/2.6

Table 1